Chapter 8

Summary and Conclusions

During the passive seismic experiment BOHEMA (2002/2003) in the western Bohemian Massif, a large data set was obtained, which was analysed with the *P* and *S* receiver function methods. The aim was to obtain images of the discontinuities in the Earth's lithosphere (Moho, lithosphere-asthenosphere boundary) and upper mantle ('410' and '660') beneath the western Bohemian Massif. The investigated region is characterized by the occurrence of earthquake swarms, emanation of upper-mantle derived CO_2 in mineral springs and mofettes, Tertiary and Quaternary volcanism, and neotectonic crustal movements. To explain these phenomena, the existence of active magmatic reservoirs near the crust-mantle boundary has been suggested in the past. In the geologically comparable regions of the Eifel and French Massif Central, tomography studies imaged plume-like structures which were suggested to also exist beneath the Bohemian Massif.

Figure 8.1 gives an overview about the *P*-to-*S* converted phases observed at stations of the BOHEMA experiment. Phases that can be clearly identified are conversions from the Moho, multiple reverberations within the crust, and the converted phases from the discontinuities of the mantle transition zone at 410 and 660 km depth. Furthermore there are indications for a conversion from the still-debated discontinuity at 520 km depth.

For investigation of the lithosphere-asthenosphere transition, *S*-to-*P* converted phases were also analysed. The data set was complemented by data from an earlier seismic experiment by *Geissler et al.* (2005).

The results obtained for the various discontinuities are summarized in this chapter 'from top to bottom'. Finally, a model is shown that incorporates the results and may help during the ongoing discussion about the existence of a "baby plume" and/or asthenospheric updoming beneath the investigation area.

8.1 Moho depths and crustal v_p/v_s ratios beneath the western Bohemian Massif

By analysis of more than 5000 *P* receiver functions recorded at 110 broad band and short period seismic stations of the BOHEMA experiment, crustal thickness beneath each station could be calculated. This results in the highest resolution Moho map of this large area until now. The map of Moho depths is displayed in Figures 5.8 and 5.9. It shows crustal thicknesses of 27 to 31 km in the Saxothuringian unit, 30 to 33 km in the Teplá-Barrandian and 34 to 39 km in the Moldanubian unit east of the Bavarian Shear Zone. A dominant feature in the Moho depth map is an area of thin crust of about 26 to 28 km beneath the western Eger Rift. The internal geometry of this updoming seems to be irregular: crustal thickness gradually increases towards the ENE to „normal“ values of about 31 km, whereas towards the WSW there seems to be an abrupt depth increase from 26 to 31 km. This apparent Moho updoming was already observed with less resolution by *Geissler et al.* (2005). It corresponds well with the area of CO_2 degassing fields at surface. The main swarm earthquake area of Nový Kostel is situated at the northeastern margin of the Moho updoming area. The Moho depth increases towards the SE and reaches values of almost 40 km between the Central Bohemian and the Bavarian Shear Zones. This result is in good agreement with former seismic studies and compilations (e.g. *Hrubcová et al.*, 2005; *Wilde-Piórko et al.,* 2005; *Dèzes and Ziegler*, 2001). The Moho depth values have an estimated uncertainty of ± 2 km.

Furthermore, a map of average crustal v_p/v_s ratios is presented for the investigation area (Figure 5.7). Before, v_p/v_s ratios were only provided for selected locations (e.g. *Geissler et al.*, 2005). The v_p/v_s ratios were obtained with the grid search method by *Zhu and Kanamori* (2000) for 34 stations of the BOHEMA experiment with clear Moho *Ps* conversions and crustal multiples (Table 5.1, Figures 5.4 and 5.6). The values vary between 1.66 and 1.81, with an average value of 1.73. For the remaining stations, the investigation area was divided into subareas associated with the Variscan tectonometamorphic units of the Bohemian Massif. For these subareas, mean values of v_p/v_s ratios and their standard deviations were calculated of the single values obtained with the method by *Zhu and Kanamori* (2000). The resulting map (Figure 5.7) displays a relatively high mean v_p/v_s ratio of 1.75±0.02 for the Saxothuringian part of the Bohemian Massif. To the southeast, the northern part of the Teplá-Barrandian forms an area of mean v_p/v_s ratio of 1.71±0.03. The transition of the Central Bohemian Shear Zone has a higher value again of 1.75±0.03. This corresponds to results by *Hrubcová et al.* (2005) who report a v_p/v_s ratio of 1.76 in the upper crust in the vicinity of the Central Bohemian Shear Zone. Station PRU near Prague stands alone with a rather low value of 1.66±0.06. In the Moldanubian unit southeast of the Central Bohemian Shear Zone, an area of low v_p/v_s ratio of 1.69±0.05 was obtained. In the Moldanubian region west of the Teplá-Barrandian unit, the mean v_p/v_s ratio is 1.72±0.02. Finally, the region southwest of the Bohemian Massif which is covered by Mesozoic sediments, displays a mean v_p/v_s ratio of 1.72±0.04.

High values of v_p/v_s beneath the western Erzgebirge mountains reported by *Geissler et al.* (2005) could partly be confirmed (stations WERN, BG25), as well as low values at the Czech-German border east of KTB (station B17).

One possibility to explain low v_p/v_s ratios at station PRU near Prague (1.66±0.06) and in the Moldanubian region between Central Bohemian and Bavarian Shear Zone (1.69±0.05) might be the existence of quartz rich rocks beneath the stations (*Christensen*, 1996).

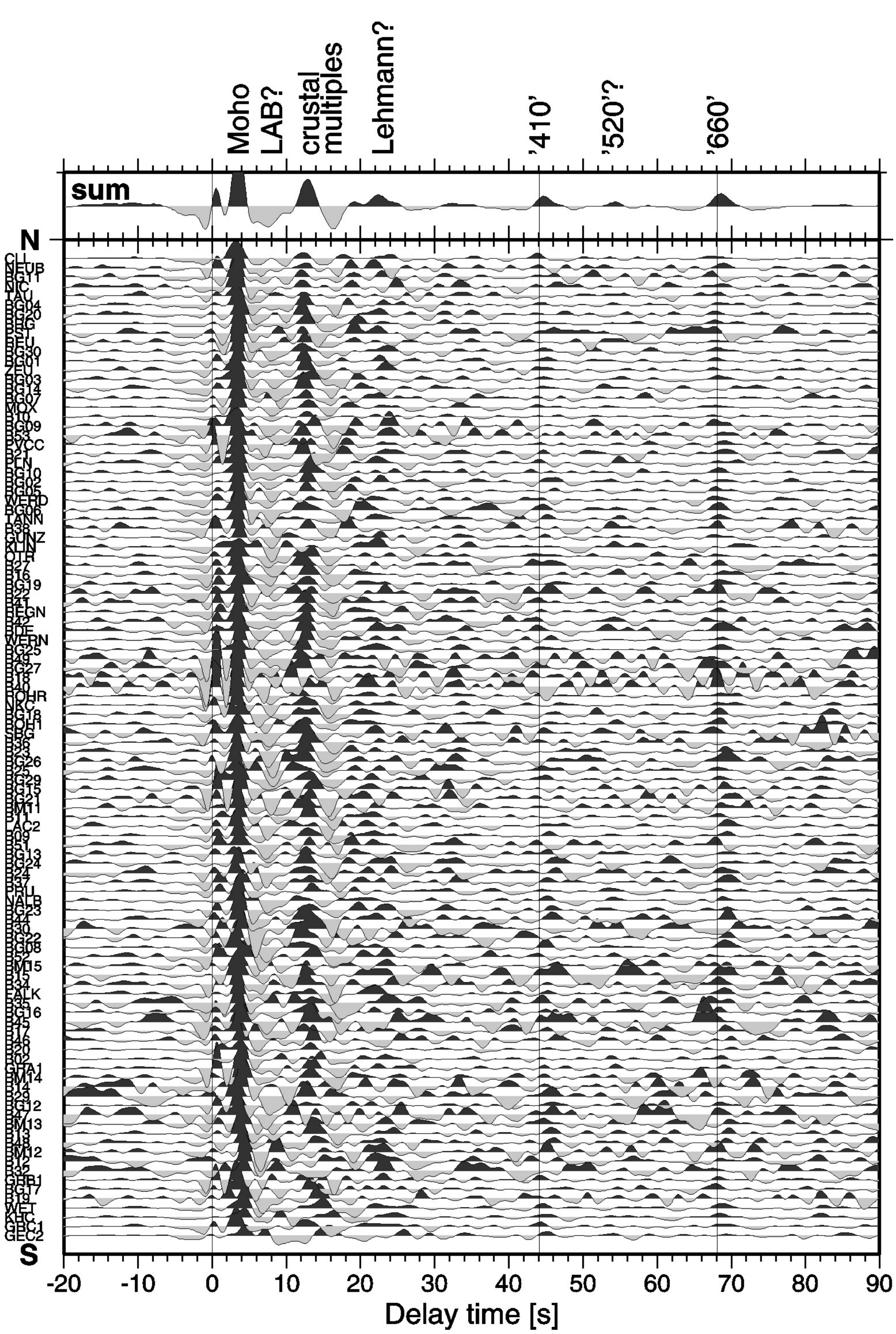

Figure 8.1: Sum traces of all stations of the BOHEMA experiment that were used for *P* receiver function analysis. The horizontal axis gives the differential time between the *P*-to-*S* converted phases and the *P* onset (zero time). Before stacking, the individual traces were filtered between 2 and 20 s and corrected for distance moveout. Stations are sorted from south (bottom) to north (top). On top of the figure, the sum trace of all individual traces is shown together with an interpretation of the observed converted phases. The phases that can be clearly identified are conversions from the Moho, multiple reverberations within the crust, and the converted phases from the '410' and '660'. Furthermore there are indications for a conversion from the still-debated discontinuity at 520 km depth. The negative signal at approximately 8 s delay time in the sum trace and the positive signal at approximately 23 s might perhaps be associated with the lithosphere-asthenosphere boundary and the Lehmann discontinuity, respectively. However, further tests are necessary to allow these interpretations.

8.2 Structure and thickness of the lithospheric mantle

In the area of Moho updoming and mantle-derived CO_2 emanations another interesting feature was observed in the *P* receiver functions: a positive phase at about 6 s delay time with respect to the *P* onset, followed by a strong negative phase at about 7 to 8 s. A mapping of the occurrence of these additional phases showed that they form a coherent structure centred on the western Eger Rift (Figure 6.1). While the positive phase near 6 s was already observed by *Geissler et al.* (2005), the negative phase at 7.5 s was not - probably due to too sparse data. However, in this thesis the negative phase turns out to be larger in amplitude than the positive phase near 6 s and to cover a larger area of 5300 km^2, which includes the occurrence of the positive "*6 s phase*" (*Geissler et al.*, 2005) as a subarea in the central and eastern part of the pink shaded area in Figure 6.1. A test of the distance moveout behaviour of the two additional phases indicates that they are direct conversions rather than multiple reverberations, meaning that they image a structure in the uppermost mantle rather than within the crust. However, as moveout effects at such shallow depths are not very strong, the indications are only weak and thus not very reliable.

The phases at 6 s and 7.5 s can be modelled by a velocity increase at 50 km suggested by results of seismic reflection and refraction investigations (*Hrubcová et al.*, 2005; *Tomek et al.*, 1997) and by a velocity decrease at 65 km depth. The velocity decrease might be explained by local asthenospheric updoming and/or a confined body of partial melt, which might be the cause for high CO_2 mantle fluid flow and earthquake swarm activity in this presently nonvolcanic, intracontinental rift area.

An updoming of the lithosphere-asthenosphere boundary had already been proposed earlier by *Babuška and Plomerová* (2001). However, their suggested lithospheric thickness of 80 to 90 km beneath the contact of Saxothuringian and Moldanubian unit would be considerably deeper than the 65 km suggested by the *P* receiver function data shown here. Asthenospheric upwelling beneath the western Eger Rift is also indicated by e.g. *Faber et al.* (1986), *Plomerová and Babuška* (1988), *Passier and Snieder* (1996), and *Plomerová et al. (1998).*

To test the idea of lithospheric thinning and to map the lithosphere-asthenosphere boundary in the west Bohemia region, an analysis of *S*-to-*P* converted phases (*S* receiver function method) was carried out in this thesis. The data show a very clear Moho signal approximately 3 to 4 s delay time after the *S* onset, corresponding very well to the delay time obtained by *P* receiver function analysis. After the Moho *Sp* conversion, a coherent negative phase arrives at 8 to 10 s and for the southern Moldanubian part at 12 to 14 s. The possibility of the negative signal being merely a side lobe of the Moho signal and thus an artefact produced by the deconvolution is ruled out by a test that compares the side lobes of the deconvolved *P* and *SV* signals. Therefore it is concluded that the negative signals observed in the *S* receiver functions at 8 to 14 s are most probably the *S*-to-*P* converted phases generated at a negative velocity gradient, which might be interpreted as the lithosphere-asthenosphere transition (LAB). However, from previous research this transition is not very well constrained yet regarding its nature, depth location and width of gradient zone (see Chapter 6).

An approximation of the depth origin of the negative phase was achieved by multiplying the picked delay time by a factor of 9 based on the *IASP91* standard earth model (*Kennett*, 1991; *Kennett and Engdahl, 1991*). The results are displayed in Figure 6.12. If the negative gradient is interpreted as the lithosphere-asthenosphere transition, the map in Figure 6.12 shows lithospheric thickness of 80 to 90 km beneath the Saxothuringian and partly the Teplá-Barrandian unit. Towards the south, the thickness strongly increases in the Moldanubian part of the investigation area to 115 to 135 km. For the Saxothuringian unit in the north, *Babuška and Plomerová* (2001) obtained a slightly thicker lithosphere of 90 to 120 km, while their thickness of 120 to 140 km in the Moldanubian unit (Figure 2.5) agrees very well with the values obtained in this thesis. The transition from the Saxothuringian/Teplá-Barrandian LAB in the north to the Moldanubian LAB in the south does not show a single clear negative peak but seems to represent a transition from the thinner to the thicker lithosphere with partly doubling of the negative signals. *Babuška and Plomerová* (2001) interpret the patterns of *P* wave residuals and shear wave splitting parameters in the transition from the Saxothuringian to the Moldanubian as possible underthrusting of a part of the Saxothuringian subcrustal lithosphere beneath the Moldanubian or a hypothetical remnant of the Early Palaeozoic oceanic lithosphere subducted to the south during collision of the Saxothuringian and Moldanubian units.

However, a clear asthenospheric updoming beneath the contact of the Saxothuringian and Moldanubian units centred beneath the western Eger Rift as suggested in *P* receiver function data, cannot be stated from *S* receiver functions.

Two scenarios can be imagined to explain the occurrence of the negative phase in the *P* and *S* receiver functions at different depths (Figure 8.2):

1) The negative phases in the *P* and *S* receiver functions represent two distinct discontinuities. A thin low velocity layer is detected by the *P* receiver functions in the lithospheric mantle at approximately 65 km depth. As its thickness is between 2 and 6 km, it can not be detected by the *S* receiver function method. This low velocity layer could for example be caused by patches of partial melt. As the negative phase in the *P* receiver functions is observed in the area of CO_2 degassing and occurrence of earthquake swarms, a causal connection between the low velocity area at 65 km depth and these phenomena might be assumed. The negative gradient observed in *S* receiver function data at approximately 9 to 10 s is more or less coherent throughout the whole profile and might thus be interpreted as the lithosphere-asthenosphere transition. However, the thinning of the lithosphere proposed by *Babuška and Plomerová* (2001) would then not be obvious in the *S* receiver function data, furthermore the diapiric mantle upwelling suggested by *Granet et al.* (1995) for the Bohemian Massif would show no imprint on the lithosphere-asthenosphere transition.

2) The negative phases in the *P* and *S* receiver functions represent in principle the same negative velocity gradient, but strongly influenced by the different frequency contents of the *P* and *S* waves and by the possible nature of the transition from high to low velocities with increasing depth. For example, if the gradient is steep at about 70 km depth and becomes increasingly less steep at 80 to 90 km depth, then *P* receiver functions would image the steep part while *S* receiver functions would

image also the flatter part of the gradient. However, as the negative phase in the *P* receiver functions is only observed in the broader surroundings of CO_2 degassing at surface and earthquake swarm occurrence, the proposed steep gradient zone would also occur only in this area. Again, this implies a thin region of strongly decreased seismic velocity at about 65 km depth which might be associated with the occurrence of partial melts at this depth range.

8.3 Upper mantle discontinuities at 410 and 660 km depth

The sum trace of all individual *P* receiver functions used in this study shows a slightly increased delay time for the *Ps* conversions from both the '410' and '660' compared to the *IASP91* global reference model (*Kennett*, 1991; *Kennett and Engdahl*, 1991) (see Figures 7.5 and 7.6). The '410' shows a delay time increased by +0.7 ± 0.2 s, while the delay time of the '660' is increased by +0.5 ± 0.2 s.

Looking in more detail at the two discontinuities, both show a slightly deepening trend towards the south (Figures 7.7 and 7.8). In the north and northeast of the investigated area, the values do not significantly differ from the values predicted by the *IASP91* reference model. The largest delay times are measured in the southernmost part of the sampled area, i.e. beneath the Austrian Alps with values increased by +0.7 to +1.5 s for the '410' and +1.5 s to +2.9 s for the '660' in relation to *IASP91*. However, data coverage is not very dense in this area so that the values are not reliable.

A low velocity layer atop the 410-km discontinuity as suggested by some previous studies was not observed in this thesis. Only very few non-coherent patches of the investigated area show such a velocity reduction.

The difference between the delay times of the '410' and '660' do not significantly differ from the value predicted by the *IASP91* global reference model. That means that the thickness of the mantle transition zone is neither increased nor decreased and thus points to normal temperatures in this depth area. This is supported by observations of *Grunewald et al.* (2001) who also found no deviations of the depths of the '410' and '660' in the area investigated in this thesis. The diapiric mantle upwelling beneath the western Bohemian Massif predicted by *Granet et al*. (1995) would thus have no impact on the topography of the 410- and 660-km discontinuity. If such a mantle finger exists, it is either too narrow to be detected by teleseismic receiver functions (diameter significantly smaller than 150 km at the depth of the mantle transition zone), or it should have its origin above the mantle transition zone.

Most probably, the slightly increased delay times of the signals from the '410' and '660' are caused by an increased v_p/v_s ratio in the upper mantle above the mantle transition zone. This means that the '410' and '660' really are located at 410 and 660 km depth, but their conversion signals experience some relative delay when they pass the layers above. As the *IASP91* global reference model does not contain an asthenosphere, an increased v_p/v_s ratio within an existing asthenosphere beneath the investigation area might explain at least some part of the observed time delay of the discontinuities of the mantle transition zone.

Furthermore, a coherent *Ps* conversion is observed in the boxes of *P* receiver function data and in the sum trace at 54.4 s (Figures 7.5 and 7.6). It might be attributed to the so-called 520-km discontinuity. However, the phase was not analysed in more detail.

8.4 Model of the lithosphere and upper mantle beneath the western Bohemian Massif

Finally, two models are shown that summarize the results about location and topography of seismic discontinuities within the lithosphere and upper mantle (Figure 8.2). The models differ in their interpretation of the negative phases in the *P* and *S* receiver functions in the mantle lithosphere.

As the models combine all discontinuities observed with *P* and *S* receiver functions in this study, it becomes clearer that the area of Moho updoming beneath the western Eger Rift, the possible occurrence of additional high and low velocity zones and the transition from thinner lithosphere of the Saxothuringian/Teplá-Barrandian units to the thicker lithosphere of the Moldanubian unit coincide vertically. The occurrence of a low velocity layer at about 65 km depth ends to the south just where the steep increase in lithospheric thickness occurs. The models furthermore shows no topography of the discontinuities at 410 and 660 km depth. A slight deepening of both discontinuities in the south is indicated, but more data are necessary to confirm or deny this trend. Furthermore, a phase that might be interpreted as a discontinuity at 520 km depth within the mantle transition zone has been observed.

A comparison with the crustal and uppermost mantle model along the seismic refraction profile CEL09 suggested by *Hrubcová et al.* (2005) (see Figure 2.3) shows that the thickness of the crust of the Moldanubian unit agrees very well with the almost 40 km found in this thesis. However, crustal thickness for the Saxothuringian unit differs in the two models as *Hrubcová et al.* (2005) suggest a strong velocity contrast on top of a lower crustal layer at about 26 to 28 km depth and a gradual Moho transition at about 35 km depth. In this thesis, a crustal thickness of 27 to 31 km was obtained for the Saxothuringian unit, while there were generally no indications for the existence of a further strong discontinuity within the crust (Figure 5.10).

The model of the lithosphere beneath the western Eger Rift obtained by *Geissler et al.* (2006) (see Figure 2.8) shows an updoming of the Moho beneath the western Eger Rift that could be confirmed and mapped in more detail by the present study. It turned out that this Moho updoming seems to have an irregular internal geometry. While in *Geissler*'s model a positive converter at about 55 km depth is the most pronounced structure in the subcrustal mantle beneath the western Eger Rift, in this thesis an additional negative phase was observed that extends over a larger area and probably corresponds to a negative gradient (LAB?) at about 65 km depth. A local asthenospheric updoming with steep flanks as indicated in *Geissler*'s model does not seem likely from viewpoint of this thesis. However, the top of *Geissler*'s asthenospheric updoming corresponds to the relatively shallow depth of about 65 km at which indications for a steep negative velocity gradient was found within *P* receiver functions in this thesis.

A comparison with the model of the lithosphere beneath the western Bohemian Massif presented by *Babuška and Plomerová* (2001) (see Figure 2.5) shows that the model correlates well with the lithospheric thickness found in this thesis. However, the increase in thickness from the Saxothuringian to Moldanubian lithosphere obtained here is much steeper than in the model by *Babuška and Plomerová* (2001). However, the nature of this "step" is not clear. Some of the data obtained in this study show a doubling or broadening of the negative signal (Figure 6.13; boxes 21 and 22 in Figure 6.10a), which could point to either an abrupt increase of lithospheric thickness, or a very steep slope, or possibly even a structure from palaeosubduction within the lithosphere of this part of the investigated area. *Babuška and Plomerová* (2001) observed a mixture of anisotropic characteristics of the Saxothuringian and the Moldanubian unit within the lower lithosphere at the transition from the Saxothuringian to the Moldanubian unit. They suggested underthrusting of a part of the Saxothuringian subcrustal lithosphere beneath the Moldanubian or a hypothetical remnant of the Early Palaeozoic oceanic lithosphere subducted to the south during collision of the Saxothuringian and Moldanubian units.

Present strong CO_2 emanations of upper mantle origin, Moho updoming beneath the western Eger Rift and Tertiary/Quaternary volcanic activity comparable to the Eifel region and French Massif Central demand an explanation for these phenomena, like for example the assumption of a diapiric mantle upwelling ("baby plume") as suggested by *Granet et al.* (1995) (see Figure 2.6) and/or the existence of magmatic reservoirs near the crust-mantle boundary as suggested by e.g. *Weinlich et al.*, 1999, *Bräuer et al.*, 2005 or *Geissler et al.*, 2005. However, the seismic discontinuities of the lithosphere and upper mantle beneath the western Bohemian Massif as observed in this study do not give rise to the assumption of a "baby plume" beneath the western Bohemian Massif. On the other hand, the possible existence of such a structure in the upper mantle above the mantle transition zone could not be completely ruled out. Teleseismic tomography carried out with the BOHEMA data set also does not show clear indications for a plume-like structure (*Plomerová et al.*, 2006, submitted). Nevertheless the observation of a negative velocity gradient at 65 km depth in this study suggests the presence of relatively hot mantle material with decreased *S* wave velocity, or even partial melts within the lithosphere, which might be the cause of at least some of the described phenomena beneath the western Bohemian Massif.

Figure 8.2 (next page): Cartoon of the seismic discontinuities beneath the western Bohemian Massif as observed in this study. The section represents a NNW-SSE profile across the western Eger Rift (ER) with true proportions. TB is the Teplá-Barrandian unit. With increasing depth, the aperture of the rays allows to observe a larger area, however with less resolution. At approximately 30 km depth the Moho is observed, with an updoming beneath the western Eger Rift to approximately 27 km and deepening towards the Moldanubian. The thin black line beneath the western Eger Rift represents a velocity increase at about 50 km depth, which was modelled from the local occurrence of a positive phase near 6 s delay time in *P* receiver functions. In the *P* and *S* receiver functions, negative phases are observed at about 7.5 s and 9 to 10 s, respectively. They can for example be interpreted as two distinct structures with negative velocity gradients (**a**), or as one single discontinuity with changing steepness of gradient, so that the different wave types image the part of the gradient that they are most sensitive to (**b**). The negative gradient observed in the *S* receiver functions was interpreted as lithosphere-asthenosphere boundary in this study. At the transition to the Moldanubian unit, lithospheric thickness strongly increases. However, a clear image of the nature of this increase could not be obtained. Furthermore, the angle of the contact between Saxothuringian (I) and Moldanubian lithosphere (II) is not known.
The upper mantle discontinuities at 410 and 660 km depth do not show any significant topography apart from a slight deepening in the southernmost part of the area. A phase at 54.4 s delay time observed in *P* receiver function data might perhaps be interpreted as the 520-km discontinuity. The possible existence of a plume-like velocity anomaly in the upper mantle above the mantle transition zone cannot be completely ruled out by this study.

(a)

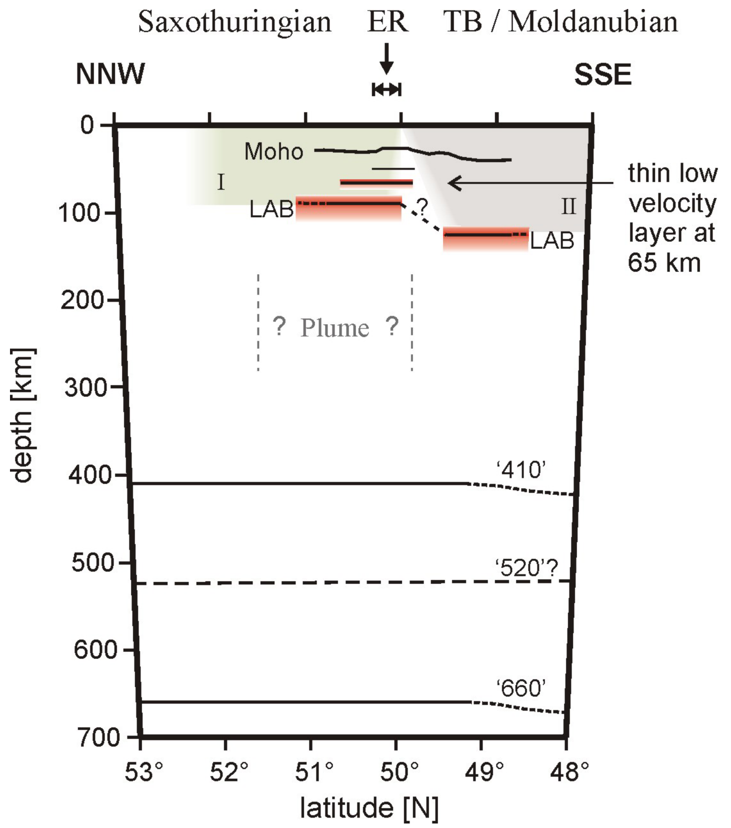

I: Saxothuringian lithosphere

II: Moldanubian lithosphere

(b)

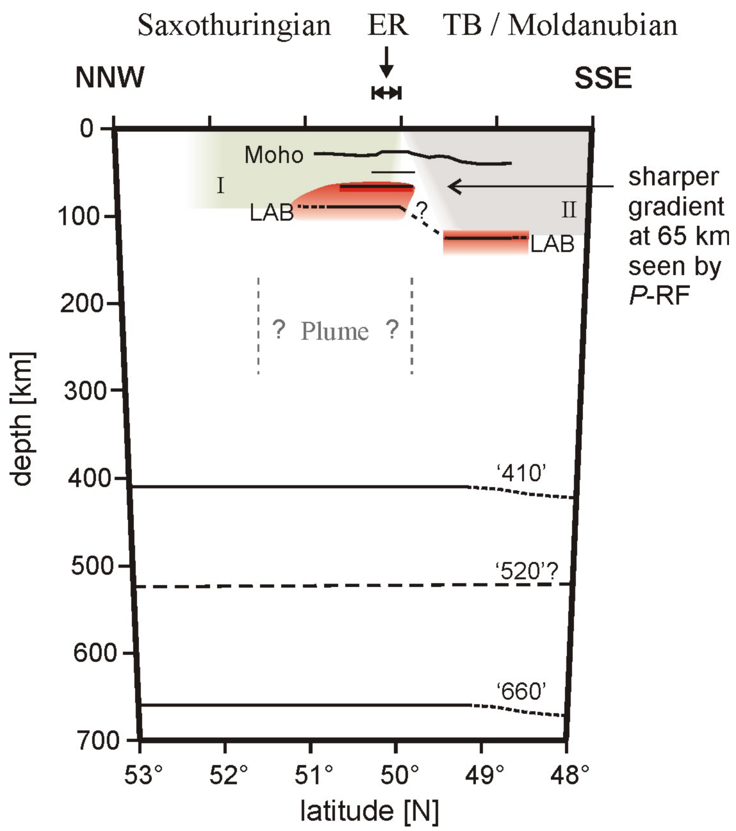

8.5 Open questions/ Outlook

As usual, during the effort to answer one question, many other questions arise. Furthermore, many aspects that need to be investigated could not be touched within the frame of this work.

Synthetic tests and modelling of the observed phases within the lithospheric mantle at 6 s and 7.5 s delay time and of the lithosphere-asthenosphere transition are necessary in order to decide which of the suggested scenarios for the velocity reduction in the lithospheric mantle is more probable.

The receiver function investigation presented in this thesis has been carried out under the assumption of isotropic, horizontal layers beneath the western Bohemian Massif. This is, of course, a simplification of the real situation. From anisotropy studies it is known that the lithospheric mantle beneath the western Bohemian Massif shows anisotropy (e.g. *Babuška and Plomerová*, 1993, 2001; *Plomerová et al.*, 1998, 2002, 2006). A future task could thus be the investigation of anisotropy or dipping layers within the receiver function data by investigating azimuthal behaviour and by using also *T* components of rotated and deconvolved seismograms.

The Moho depth map obtained within this thesis revealed a rather steep increase in Moho depth across the Central Bohemian Shear Zone (Figure 5.10). This and the continuation of Moho depth from the Moldanubian to the southwest across the Bavarian shear zone should be investigated in more detail with the receiver function technique with more seismic stations. The station distribution of the BOHEMA experiment did not provide enough data to answer this question. Ongoing projects of Czech and Austrian colleagues will hopefully make it possible soon.

Recent results regarding the composition and flux rates of CO_2 emanations with signature of subcontinental lithospheric mantle indicate that there are very recent changes and dynamics observable (*Bräuer et al.*, 2005; *H. Kämpf, personal communication*), which points to presently active magmatic processes in the uppermost mantle beneath the intersection area of Eger Rift and Regensburg-Leipzig-Rostock zone. In order to even better resolve possible magmatic underplating or the occurrence of partial melts that might lead to the described processes, an extremely dense network or profiles of seismometres within this region (station spacing 2 to 3 kilometres) might help to map the fine structure of the Moho as well as seismic discontinuities within the lithospheric mantle.

Magnetotelluric sounding, which has been used to estimate the depth of the lithosphere-asthenosphere transition, should also be able to detect partial melting above or below the crust-mantle boundary. Therefore magnetotelluric measurements within the investigation area might be helpful to test the existence and depth location of areas of partial melt within the lithosphere.

In order to better constrain the location of the lithosphere-asthenosphere transition and of the discontinuities at 410 and 660 km depth, more data from stations in eastern and southern Bavaria have to be included. As most of the teleseismic events have northern to eastern backazimuths, the investigation area would then show better data coverage than in the present thesis. As current research aims at a better knowledge of lithospheric thickness beneath Europe, it will be possible to compare and connect the results of this thesis with the future results of research.

Receiver functions obtained with the BOHEMA data set also show indications of *P*-to-*S* converted phases from the base of the asthenosphere (Lehmann discontinuity) and from the discontinuity at 520 km depth. However, the signal from a possible Lehmann discontinuity probably interferes with multiples from the Moho and lithosphere-asthenosphere boundary. If it exists, it might be better constrained with the *S* receiver function method. However, the *S* receiver functions analysed in this thesis for the lithosphere-asthenosphere transition do so far not give hints to a *S*-to-*P* converted signal from the Lehmann discontinuity. The data has to be analysed in more detail. To further constrain the existence and depth of the '520', synthetic tests are necessary.

Finally, future research in this area would certainly benefit from further comparison or parallel research activities in the Eifel volcanic fields and French Massif Central.